Hydrothermal Gelation of Pure Cellulose Nanofiber Dispersions

*Shin Suenaga and Mitsumasa Osada**

Department of Chemistry and Materials, Faculty of Textile Science and Technology, Shinshu University, 3-15-1, Tokida, Ueda, Nagano 386-8567, Japan

KEYWORDS: Cellulose nanofiber, Wet pulverization, Hydrothermal treatment, Gelation mechanism, Mechanical strength, Chemical-free synthesis method

ABSTRACT. Gelation of cellulose nanofibers (CNFs) through conventional crosslinking or reprecipitation requires the use of additives. Here, for the first time, the gelation of pure CNF dispersions has been achieved solely by mechanical disintegration and a hydrothermal process without chemical modification. Different concentrations of cellulose powder were dispersed in water, following which these CNF dispersions were subjected to hydrothermal treatment at 160 °C for different lengths of times in a sealed reactor. Self-sustaining hydrogels with no discoloration were obtained. The chemical properties and crystal structures of the CNFs were essentially unchanged following hydrothermal treatment. Although the molecular mass of the cellulose was slightly lower after hydrothermal treatment, the polymer density of the cellulose at the same hydrodynamic radius was unchanged after hydrothermal treatment. Hence, chemically crosslinked

structures did not form during the hydrothermal process. Instead, physical network structures developed within the CNF hydrogels, which increased the mechanical strength. Moreover, this network structure and therefore the strength of the hydrogel could be improved by increasing the mechanical disintegration time or the cellulose concentration of the CNF dispersion. To ensure sufficient hydrothermal gelation, it was important that the CNF dispersion had a storage modulus greater than 20 Pa.

1. INTRODUCTION

The ultimate biomaterial will be able to be prepared using only water and a biomass resource, without additional chemical modification. Chemical modification is a useful way to control the shape and strength of biomaterials, as it is an easy way to achieve the requisite homogeneous dispersions of biomass material in water. If chemical modification is not performed, and no additives are used, dispersion requires the use of physical force. One possible means of accomplishing this is wet pulverization with a water jet, which can disintegrate biomass particles into nanofibers (NFs).[1–5] The physicochemical properties of NF dispersions, such as transmittance and viscosity, can be controlled through disintegration time; however, NF dispersions prepared in this manner cannot maintain a constant shape due to their flowability.[6–9]

Herein, we propose hydrothermal gelation as a means to confer shape stability to NF dispersions after disintegration. Polysaccharide NF dispersions can be gelated by simply heating them in a sealed reactor. This is referred to as hydrothermal treatment, as it uses water in the pressurized liquid phase (above 100 °C). Hydrothermal gelation has been carried out previously with 2,2,6,6-tetramethylpiperidine-1-oxyl (TEMPO)-oxidized cellulose nanofibers (TOCNs) and α- and β-chitin nanofibers (ChNFs), although many aspects of the process remain unclear.[10,11] In particular, the mechanism of

gelation and the impacts of NF morphological features, molecular mass, and NF concentration on the mechanical strength of the resulting hydrogel are not well understood. In this study, cellulose, which is the most abundant biomass material, was converted to a self-sustaining hydrogel through wet pulverization and hydrothermal gelation. In addition, the gelation mechanism and physicochemical properties of the hydrogels were completely elucidated.

2. EXPERIMENTAL SECTION

2.1. Materials and preparation of cellulose nanofibers (CNFs)

Microcrystalline cellulose powder (W-300G) with an average particle size of 28 μm was obtained from Nippon Paper Industries Co., Ltd. (Tokyo, Japan) and used without further purification. Acetone, methanol, *N*,*N*-dimethylacetamide (DMAc), *tert*-butyl alcohol, hydrochloric acid, sulfuric acid, potassium bromide, and lithium chloride were purchased from Wako Pure Chemical Industries (Osaka, Japan) and used without further purification. A polystyrene standard (molecular mass = 105,000) was purchased from Malvern Panalytical, Ltd. (Malvern, UK) and used as a calibrant for size exclusion chromatography (SEC).

Scheme 1 shows the steps involved in the wet pulverization and hydrothermal gelation process used to obtain cellulose nanofiber (CNF) hydrogels. CNF dispersions were initially prepared at a concentration of 1 wt.% and subjected to mechanical disintegration with a ceramic ball for 50 collisions (called "passes" hereafter). A cellulose powder was suspended in distilled water, then the slurry was disintegrated to form CNFs with a Star Burst Mini wet pulverizing and dispersing device (Sugino Machine Co., Ltd., Uozu, Japan) equipped with a ball-collision chamber. In the disintegration process, the slurries were pressurized at approximately 245 MPa and ejected into the device chamber through a

nozzle with an aperture of 100 μm, then pulverized with the ceramic ball.

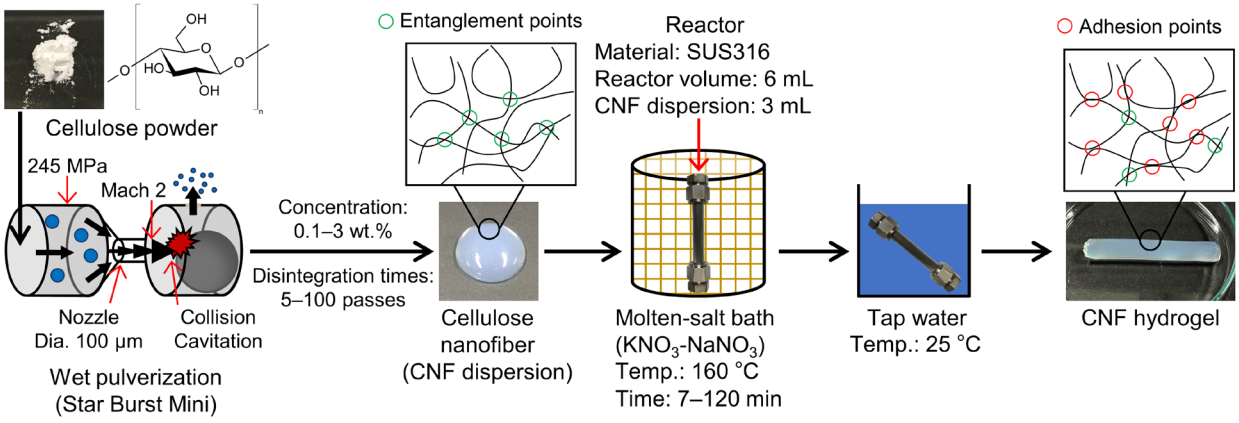

Scheme 1. Illustrations of the wet pulverization and hydrothermal gelation processes used to form CNF hydrogels.

The effects of mechanical disintegration time and cellulose concentration of the CNF dispersion on the properties and mechanical strength of the hydrogels were then systematically assessed, with either a varying number of passes (1 wt.% CNF dispersions, subjected to 5, 10, 30, 50, or 100 passes) or a varying CNF concentration (0.1, 0.3, 0.5, 1, 2, or 3 wt.% CNF dispersions, each subjected to 50 passes). The disintegrated samples were recovered after cooling them to 25 °C using a heat exchanger, and then the pH was measured with a KR5E pH meter equipped with an LE407 module (As One Corp., Ltd., Osaka, Japan). The CNF dispersions were heated at 40 °C for 10 min, then defoamed at a speed of 2000 rpm for 1 min using an ARE-250 mixer (Thinky Co., Ltd., Tokyo, Japan). This was to prevent bubble formation in the hydrogels after hydrothermal treatment or in the dispersions during dynamic viscoelastic measurements.

2.2. Gelation via hydrothermal treatment

To prepare the hydrogels, approximately 3 mL of CNF dispersion was loaded into a 6-cm^3 316-grade stainless steel tube reactor, which was subsequently immersed in a 160 °C

molten KNO_3–$NaNO_3$ bath. The saturated vapor pressure in the reactor at 160 °C was calculated as 0.62 MPa.[12] The temperature inside the reactor was measured directly by inserting a thermocouple into the reactor. For each disintegration time (number of passes) and CNF concentration tested, CNF dispersions were heated for 7, 15, 30, 60, or 120 min, which includes a warmup time of approximately 4 min.[10] After the heating process, the reactor was removed from the molten salt bath and rapidly cooled in a 25 °C water bath. The obtained hydrogel was removed from the reactor and placed in a glass dish. The pH of the CNF hydrogels was measured using the KR5E pH meter.

2.3. Field-emission scanning electron microscopy (FE-SEM) observations

The hydrogels were cut into pieces 8 mm wide and approximately 2 mm thick. The CNF dispersions and the cut hydrogel samples were immersed in *tert*-butyl alcohol for three days. After treatment with *tert*-butyl alcohol, the samples were quickly frozen and dried under vacuum (0.02 MPa) for several hours. A small piece of each dried sample was mounted on carbon tape with tweezers and coated with a 2.5-nm thick layer of osmium with a Neoc-STP osmium coater (Meiwafosis Co., Ltd., Tokyo, Japan). The coated samples were then imaged with a S-5000 FE-SEM (Hitachi, Tokyo, Japan) operated at a voltage of 5.0 kV. From the FE-SEM images, 120 CNF widths were determined using Image-J software (NIH, Bethesda, USA), and a histogram showing the frequency of widths from 2 to 60 nm was constructed. The number average width of the CNFs was determined for each disintegration time.

2.4. Optical transmittance measurements

The prepared hydrogels were ground with a pestle and mortar to obtain flowing pastes. The CNF dispersion and hydrogel pastes were each loaded directly into a quartz cuvette, and transmittance was measured from 200 to 700 nm at 25 °C on a V-530 UV-visible (UV-vis)

spectrophotometer (Jasco Co., Ltd., Tokyo, Japan) equipped with a Jasco ETC-505 Peltier-type temperature controller. Distilled water was used as a sample blank. The measurements of the 1 wt.% CNF dispersions subjected to 50 passes were performed in triplicate, and the mean and standard deviation were calculated.

2.5. Fourier-transform infrared (FTIR) spectrometry

The CNF dispersions and hydrogels were frozen at −80 °C, then lyophilized for one day with an FDU-2200 freeze-dryer (Tokyo Rikakikai Co., Ltd., Tokyo, Japan). The dried samples were blended with KBr and pressed into pellets with a mini-hand press (Shimadzu, Tokyo, Japan). FTIR spectra were obtained by performing 32 scans from 500 to 4000 cm^{-1} at a resolution of 4 cm^{-1} on a Jasco FT/IR 4200 FTIR spectrometer.

2.6. X-ray diffraction (XRD) analysis

An SSP-10A hand press (Shimadzu, Tokyo, Japan) was used to form the lyophilized CNF dispersions and CNF hydrogels into pellets of 1.3 cm diameter and 0.3 mm thick by applying 750 MPa pressure for 1 min. XRD patterns were collected from 5° to 35° (2θ) on a RINT 2500 HF/PC diffractometer (Rigaku, Tokyo, Japan) equipped with a Cu Kα radiation source (λ = 1.5418 Å) at 40 kV and 40 mA. The crystallinity index (CI) was determined by Equation 1.[13]

$$CI = (I_{200} - I_{am})/I_{200}, \quad \text{Eq. 1}$$

where I_{200} is the peak intensity in the [200] plane and I_{am} is the diffraction intensity of the amorphous phase at 18°. The *d*-spacing (Å) was calculated by Bragg's law (Equation 2).

$$d\text{-spacing (Å)} = \lambda/2 \sin\theta, \quad \text{Eq. 2}$$

where λ is the wavelength of Cu Kα radiation and θ is the scattering angle. The crystal size (CS) was determined with the Scherrer equation (Equation 3).

$$CS\ (nm) = k\lambda/\beta_0(\cos\theta), \quad \text{Eq. 3}$$

where k is a constant indicating the shape factor (0.9), and β_0 is the full width at half-maximum (FWHM) of the diffraction peak.

2.7. Size exclusion chromatography (SEC) and light scattering analysis

LiCl (2.46 g) was added to DMAc (28.3 g), and the mixture was stirred at 30 °C for 4 h to obtain a clear and colorless 8 wt.% LiCl/DMAc solution. The lyophilized CNF dispersions and CNF hydrogels were activated through a solvent-exchanging method reported elsewhere.[14,15] Each lyophilized sample (0.03 g) was immersed in 4 mL of distilled water overnight, followed by centrifugal precipitation at 10,000 g for 3 min. The supernatant was exchanged from water to acetone. This process was performed three times, and the suspensions were stored overnight at room temperature. The acetone was then exchanged to DMAc with the same solvent-exchange procedure. Finally, the solvent-exchanged samples were dried under vacuum for 24 h following decantation. Each activated sample (0.02 g) was stirred in 8 wt.% LiCl/DMAc (1.7 g) at room temperature for two days until a clear solution was obtained. After dissolution, fresh DMAc (13.5 g) was added to the solution, which was subsequently stirred for three additional days. The polystyrene standard was dissolved directly in 1 wt.% LiCl/DMAc at room temperature.

High-performance (HP) SEC paired with refractive index (RI) and light-scattering detection was employed for determination of the molecular mass distribution of the CNF dispersions and hydrogels. Samples were prepared at a concentration of 1.42 mg/mL. Sample solutions and the eluent were filtered through 0.45 μm polytetrafluoroethylene disposable membrane filters prior to SEC analysis.

The GPCmax HP-SEC system (Malvern Panalytical, Ltd.) included a high-pressure pump, an on-line degasser, an autosampler, and a TDA305 column oven. Separation was performed at 30 °C on a Shodex KD-806M SEC column (8.0 × 300 mm, Showa Denko Co., Ltd.) equipped with a Shodex KD-G guard column (4.6 × 10 mm). The injection

volume was 100 μL, and 1 wt.% LiCl/DMAc was used for elution at a flow rate of 0.5 mL/min. A 670 nm incident light source was used for light scattering detection at 7° and 90°. Data acquisition and processing (to calculate number average molecular mass, weight average molecular mass, and normalized weight fraction) were carried out with OmniSEC software (Malvern Panalytical, Ltd.). The average degree of polymerization based on number (DP_n) and weight (DP_w) were respectively calculated as the number and weight average molecular mass divided by 162, which is the mass of a repeating unit of cellulose. According to a previous report, the specific refractive index increment (d*n*/d*c*) of cellulose in 1 wt.% LiCl/DMAc is 0.131.[16]

2.8. Dynamic viscoelastic measurements

Dynamic viscoelasticity analysis was performed with 0.1, 0.3, 0.5, 1, 2, and 3 wt.% defoamed CNF dispersions processed with varying disintegration times. Measurements were carried out with a Rheologia Agent A300 coaxial double-cylinder rheometer (Elquest Co., Ltd., Chiba, Japan) equipped with a thermostatic water bath set to 25 °C. The gap between the cylinders was approximately 1.1 mm. The angular frequency sweep measurement was conducted in the linear viscoelastic region from 0.0440 to 62.9 s^{-1} at a constant strain of 0.02%. Measurements of the 1 wt.% CNF dispersion subjected to 50 passes were performed in triplicate, and the mean and standard deviation were calculated.

2.9. Atomic force microscopy (AFM)

N-type silicon wafers (~1 × 1 cm) were subjected to hydrophilic treatment prior to AFM analysis. First, each silicon wafer was immersed in 20 mL acetone for 30 min to remove grease. The degreased wafers were immersed in 50 vol.% HCl/methanol solution (20 mL) for 30 min to remove organic substances. The wafers were washed with ultrapure water until the pH of the rinses was neutral, then they were oxidized by immersion in concentrated H_2SO_4 for 30 min. The

hydrophilic Si wafers were again rinsed until neutral and stored in ultrapure water prior to use.

The 1 wt.% CNF dispersions were diluted to a concentration of 0.001 wt.% with distilled water. For each sample, one drop of diluted dispersion was deposited onto a hydrophilic Si wafer, which was then dried for 5 min in a vacuum oven at 70 °C. The samples were analyzed with a Multimode-SC AFM (Bruker, Billerica, USA) operated in tapping mode at a scanning frequency of 1 Hz in air. The tip radius of the NCHV-A cantilever was 8 nm. The oscillation resonance frequency and spring constant were 320 kHz and 40 $N \cdot m^{-1}$, respectively. Data acquisition and processing were carried out using the NanoScope IIIa software package (Veeco Instruments, New York, USA). A total of 180 CNF lengths were measured during the analysis using Image-J software (NIH). A histogram showing the frequency of CNF lengths from 100 to 4000 nm vs. frequency was constructed from ten different AFM images. The number average length of the CNFs was determined for each disintegration time.

2.10. Compression testing

The CNF hydrogels were cut with a razor into pieces 8 mm wide and approximately 5 mm thick. Compression tests were performed at room temperature on an EZ Test machine (Shimadzu, Tokyo, Japan) with a 50 N load cell at a compression rate of 1 mm/min. The breaking strength and compressive modulus at 4–8% of the initial strain were determined. Measurements of the CNF hydrogels prepared at 0.5, 1, 2, and 3 wt.% subjected to 5, 10, 30, 50, and 100 passes heated for 7, 15, 30, 60, and 120 min were performed in quintuplicate, and the mean and standard deviation were calculated.

3. RESULTS AND DISCUSSION

3.1. Physicochemical properties of CNF hydrogels following hydrothermal treatment

Robust hydrogels were obtained from the

CNF dispersions (1 wt.%, subjected to 50 passes) following hydrothermal treatment at 160 °C. Photographs of the hydrogels are shown in Figure S1 of the Supporting Information (SI). The CNF hydrogels maintained their cylindrical shape over the entire heating time. In previous reports, TOCN and ChNF hydrogels displayed brown discoloration,[10,11,17] although Lewis et al. reported hydrothermal gelation of cellulose nanocrystals at 120 °C for 20 h with no discoloration.[18] Herein, the CNF hydrogels were bluish-white with no discoloration (see Figure S1). Transmittance of the CNF hydrogels vs. heating time is shown in Figure 1A. Although transmittance decreased slightly with heating time, this was not due to discoloration. UV-vis spectra of the CNF hydrogels are shown in Figure S2A. Below transmittances of 0.1%, the wavelength did not vary with heating time. Previous reports have indicated that brown discoloration decreases transmittance at wavelengths between 400 and 700 nm.[10] Hence, the slight decrease in transmittance observed here could be attributed with certainty to increasing NF width. NF width is plotted against heating time in Figure 1B. Representative FE-SEM images and the corresponding histograms of NF width frequency distributions are shown in Figure S2B. NF widths increased with heating time, which indicated the formation of a three-dimensional network structure through adhesion among the NFs. An increase in NF width was accompanied by increased light scattering, which resulted in lower transmittance.

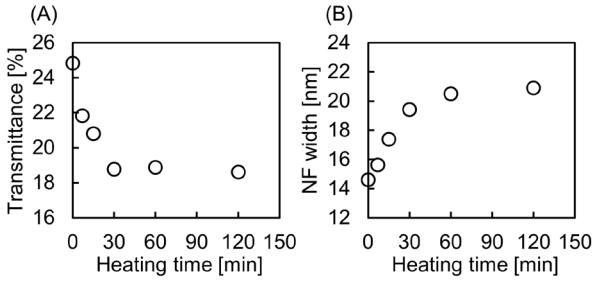

Figure 1. (A) Transmittance at λ = 600 nm and (B) number average CNF width of the CNF dispersion* and hydrogel samples (1 wt.%, 50 passes) as a function of heating time. *The CNF dispersion has a heating time of 0.

FTIR spectra of the CNF hydrogels are shown in Figure 2A. The spectra of the CNF hydrogels are identical to that of the original CNF dispersion. Overlapping FTIR spectra without offsets are shown in Figure S3. These results indicate that the chemical structure of cellulose was unchanged by hydrothermal treatment. In addition, the CNF hydrogels were likely physical gels, because no new peaks were observed. The possibility of chemically crosslinked structure formation will be discussed with the results of SEC analysis. XRD patterns from the CNF hydrogels are shown in Figure 2B.

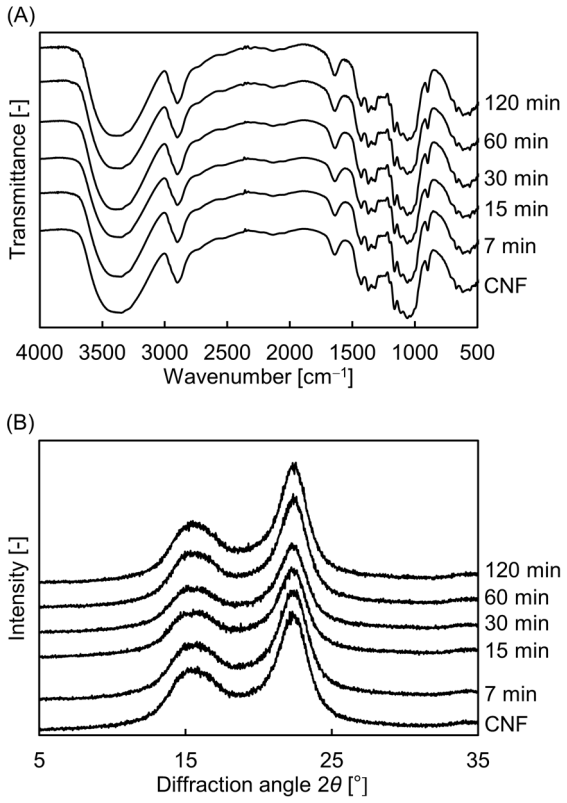

Figure 2. (A) FTIR spectra and (B) XRD patterns of CNF and hydrogel samples.

As was the case in the FTIR spectra, the XRD patterns of the CNF hydrogels were almost identical to that of the CNF dispersion. As can be seen in the FE-SEM images (Figure S2B), the NF structure of cellulose remained intact following hydrothermal treatment, indicating its crystalline structure was unchanged. It appears that hydrothermal gelation occurred through the interaction between CNFs rather than through dissolution

and subsequent reprecipitation; the latter would have resulted in transformation of the cellulose I crystalline structure to cellulose II,[19–22] but this was not observed. The crystallographic parameters of the CNF and hydrogel samples are listed in Table 1. The CI and *d*-spacing of the CNF hydrogels did not change during hydrothermal gelation, although the crystal size (CS) increased slightly with heating time. The increase in CS may have resulted from adherence between NFs. Although FE-SEM analysis showed that the NF width increased 1.5-fold as hydrothermal gelation proceeded, the increase in CS was slight.

Cellulose polymers within the CNF were regularly arranged, while those at the interfaces between adhering CNFs appeared to be randomly arranged. Adherence between CNFs is probably due to van der Waals or hydrophobic interactions rather than intermolecular hydrogen bonds, which would induce crystal formation. From these results, we propose the following two-fold mechanism for the promotion of adhesion between CNFs: the breaking of hydrogen bonds between water molecules under hydrothermal conditions enhances hydrophobic interactions between CNFs, and the promotion of CNF diffusion under hydrothermal conditions increases the contact frequency between them. However, further study is needed to verify this hypothesis.

Table 1. CI, *d*-spacing, and CS of CNF and hydrogel samples.

Heating time (min)	CI[a] (%)	*d*-Spacing (Å)	CS[b] (nm)
0	69	4.0	8.1
7	64	3.9	8.4
15	64	4.9	8.7
30	65	4.0	8.7
60	69	4.0	8.8
120	69	3.9	9.0

[a]CI: crystallinity index; [b]CS: crystal size.

The pH values of the CNF hydrogels are shown as a function of heating time in Figure 3. The pH of the hydrogels decreased to about 5 over the course of hydrothermal gelation,

although their chemical structures were unchanged (Figure 2A). Hydrolysis of glucose units in the cellulose polymer would generate organic acids via thermal decomposition. The formation of organic acids, such as acetic acid, lactic acid, glycolic acid, and malic acid, during hydrothermal treatment of saccharides has been reported.[23–26]

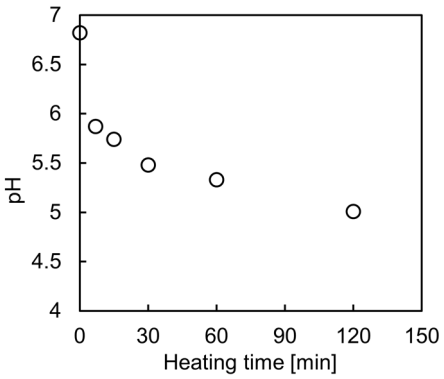

Figure 3. pH values of CNF and hydrogel samples as a function of heating time.

DP_n and DP_w in the CNF hydrogels are plotted against heating time in Figure 4A. The relationships between SEC elution volume, normalized weight fraction, and molecular mass are illustrated in Figure 4B. Both DP_n and DP_w decreased slightly with heating time. The elution profiles show that the proportion of high-molecular mass components eluted with smaller solvent volumes decreased with heating time, while the proportion of low molecular mass components eluted with larger volumes increased with heating time. In addition, the molecular mass plots showed a similar trend in relation to elution volume, regardless of heating time. Although the molecular mass plots did not overlap at the lowest elution volumes, they showed no dependence on heating time.

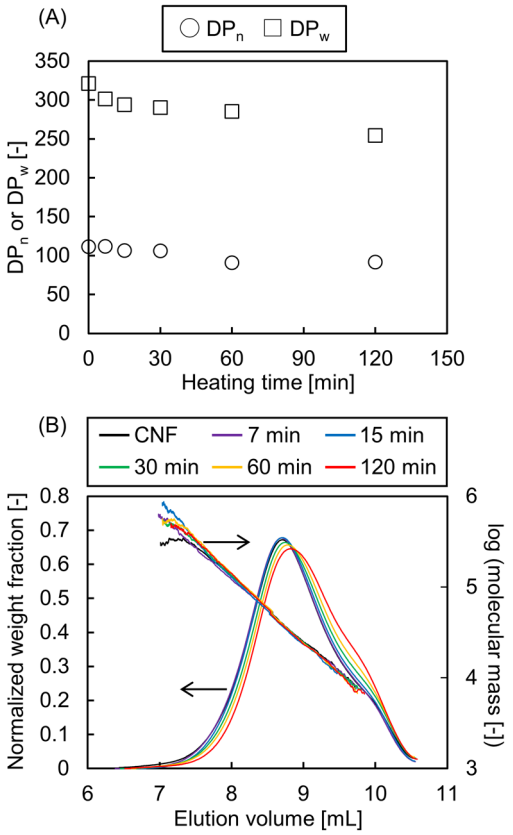

Figure 4. (A) DP_n and DP_w of CNF and hydrogel samples against heating time. (B) Relationship between the elution volume and elution pattern with respective molecular mass plots of CNF and hydrogel solutions in LiCl/DMAc.

During SEC separation, polymers are separated according to their hydrodynamic radii in the solvent, not according to molecular mass. Polymer density can be determined with the light-scattering method, even if the polymers have identical hydrodynamic radii. When hemiacetal or ester linkages form between cellulose polymers during hydrothermal treatment, the polymer density at a given hydrodynamic radius increases. An increase in polymer density is reflected by an upward shift of the molecular mass plot for a given elution volume. We did not observe such a shift and thus concluded that chemical crosslinking between the cellulose polymers did not occur. This finding was consistent with the FTIR results, thereby confirming that the CNF hydrogels formed via hydrothermal treatment were physical gels. Because the DP_n of the CNFs was approximately 100, and the glucose unit was assumed to be 0.518 nm long,[27,28] the length of the cellulose polymer was estimated to be 52 nm. The CNF subjected to 50 passes was 730 nm long, as shown in Figure 5D, which corresponds to the length of at least 10 cellulose polymers.

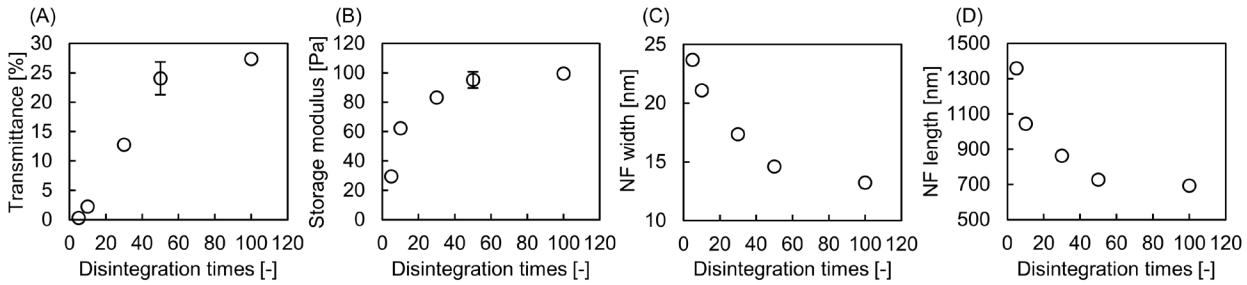

Figure 5. Properties of CNF dispersions prepared at 1 wt.% as a function of disintegration time. (A) Transmittance at λ = 600 nm, (B) storage modulus at an angular frequency of 1.26 s^{-1}, (C) number average CNF width (calculated from 120 CNF widths for each number of passes), (D) number average CNF length (calculated from 180 CNF lengths for each number of passes). In Figure 5A and 5B, the error bars show standard deviation; the measurements were performed in triplicate.

3.2. Relationship between disintegration time, physicochemical properties of CNF dispersions, and mechanical strength of CNF hydrogels

The properties of CNF dispersions prepared with different disintegration times are shown in Figure 5. UV-vis spectra of 1 wt.% CNF dispersions prepared with various numbers of passes are shown in Figure S4A. The storage and loss moduli of the CNF dispersions are plotted against angular frequency in Figure S4B. Representative FE-SEM images, histograms of NF width, representative AFM images, and histograms of NF length are shown in Figure S5. Percent transmittance (Figure 5A) and the storage moduli (Figure 5B) of the CNF dispersions both increased with increasing disintegration time. This was likely due to concurrent decreases in NF width, as shown in Figure 5C. Thinner NFs made the network structure more homogeneous, which inhibited multiple light scattering, and therefore increased transmittance. In addition, NF thickness was inversely proportional to NF number. Thinner NFs thus had more points of

entanglement, which increased the storage modulus. NF lengths are plotted against the number of passes in Figure 5D. The decrease in NF length was attributed to simple shortening of the NFs as the number of passes was increased, as opposed to hydrolysis. The disintegration process was performed under neutral conditions using only distilled water, so no acid or alkaline catalyst was present in the dispersions. In addition, the kinetic energy provided by the Star Burst system was assumed to be 18.1 kJ/mol, which is clearly less than the covalent bond energy.[29] Therefore, the average CNF length would have been reduced by tearing among the cellulose polymers, because the cellulose polymers within the CNFs were shorter than individual CNFs.

Photographs of CNF hydrogels prepared at 1 wt.% with various disintegration and heating times are shown in Figure S1. Suitability for gelation of the CNF dispersions was measured by cutting the hydrogels into pieces approximately 5 mm thick. The pieces were stood on end, and their widths were measured. The inner diameter of the reactor was 8 mm, so hydrogels >8 mm wide could not support their own gel structures. The suitability of the CNF dispersions for gelation are given in Table 2, with suitability indicated by + or – based on this criterion. The hydrogel prepared at 160 °C (7 min heating time) from the CNF dispersion subjected to five passes could not be stood upright, so further compression testing was not possible. Other CNF hydrogels produced with greater disintegration and heating times maintained their cylindrical shape.

Table 2. Suitability for gelation of CNF dispersions under various disintegration and heating conditions.

Number of passes	Heating time (min)				
	7	15	30	60	120
5	−	−	−	+	+
10	−	−	+	+	+
30	+	+	+	+	+
50	+	+	+	+	+
100	+	+	+	+	+

\+ 8-mm wide hydrogel;
− >8-mm wide hydrogel

The results of compression tests with CNF hydrogels prepared with different disintegration and heating times are shown in Figure 6A. Breaking strength (kPa) and compressive modulus (kPa) increased with increasing disintegration or heating time, then reached fairly constant values. The network structure formed by NF adhesion developed as heating time increased. The network structure connecting the NFs provided support against compressive stresses, increasing the mechanical strength of the hydrogel. Because the NF width decreased as the number of passes increased (Figure 5C), more NFs were generated with longer disintegration times, which also increased the mechanical strength. The dependence of mechanical strength on NF width and length is illustrated in Figure 6B and 6C; the mechanical strengths of the hydrogels heated for 120 min from Figure 6A are plotted against the NF widths and lengths for the corresponding number of passes from Figure 5C and 5D, respectively. Linear relationships were observed between mechanical strength and NF width as well as NF length. When the NF length or width was reduced by half, the number of NFs multiplied two- or four-fold, respectively. The increased number of NFs dispersed in water led to an increase in the mechanical strength of the resulting hydrogels.

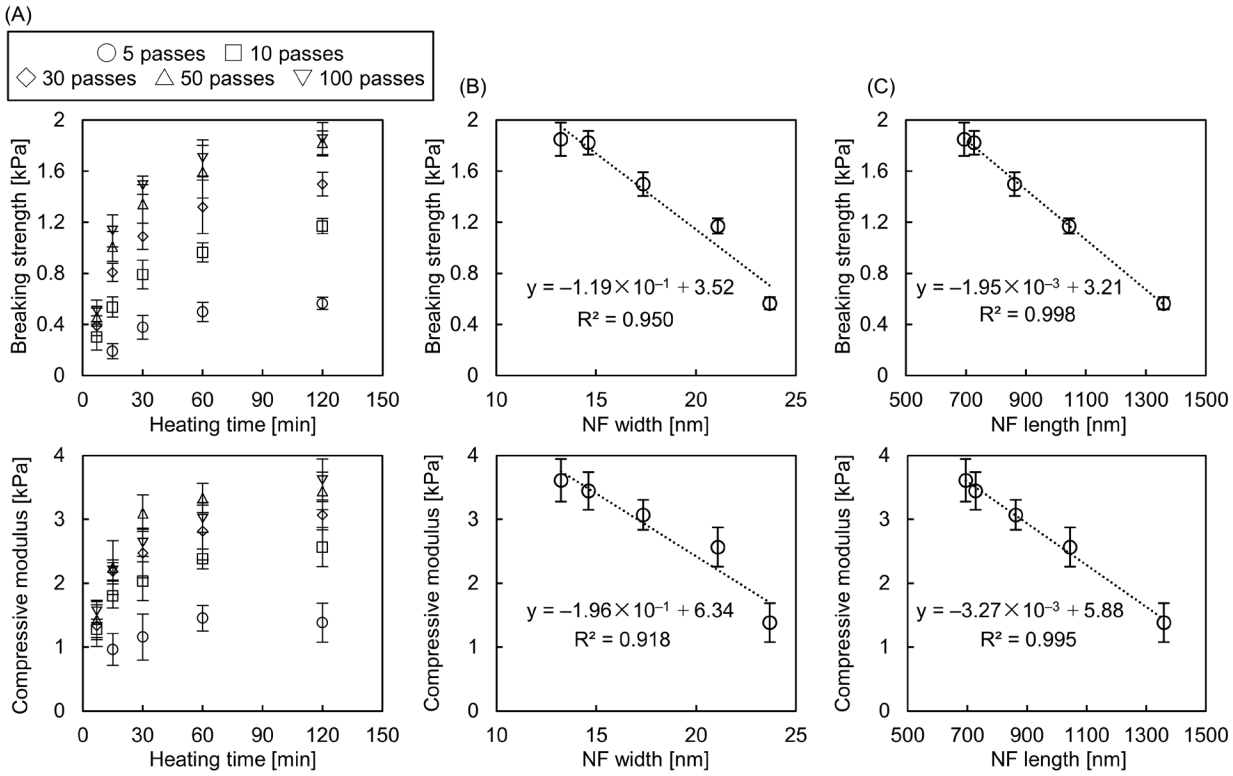

Figure 6. (A) Mechanical strength of CNF hydrogels prepared with various numbers of passes as a function of heating time. (B) Mechanical strength of CNF hydrogels as a function of NF width in CNF dispersions. (C) Mechanical strength of CNF hydrogels as a function of NF length in CNF dispersions. The mechanical strength in Figure 6B and 6C correspond to those of the hydrogels heated for 120 min in Figure 6A. In Figure 6, the error bars show standard deviation; the measurements were performed in quintuplicate.

3.3. Relationship between CNF concentration, physicochemical properties of the CNF dispersion, and mechanical strength of the CNF hydrogel

The number of NFs could be increased not only by decreasing NF width, but also by increasing CNF concentration. The relationship between the storage modulus of CNF dispersions subjected to 50 passes and CNF concentration is shown in Figure 7A. The storage and loss moduli are plotted against angular frequency in Figure S6. A network

structure consisting of entanglements between NFs developed even at a CNF concentration of 0.1 wt.%, because the storage modulus and the angular frequency were nearly independent of one another. The dependence of the storage modulus on CNF concentration followed a power rule. The slope was determined with the exponents of the values plotted in Figure 7A. The slope had a gradient of 2.1, which is the same as that reported previously for a β-ChNF dispersion prepared under neutral conditions.[30]

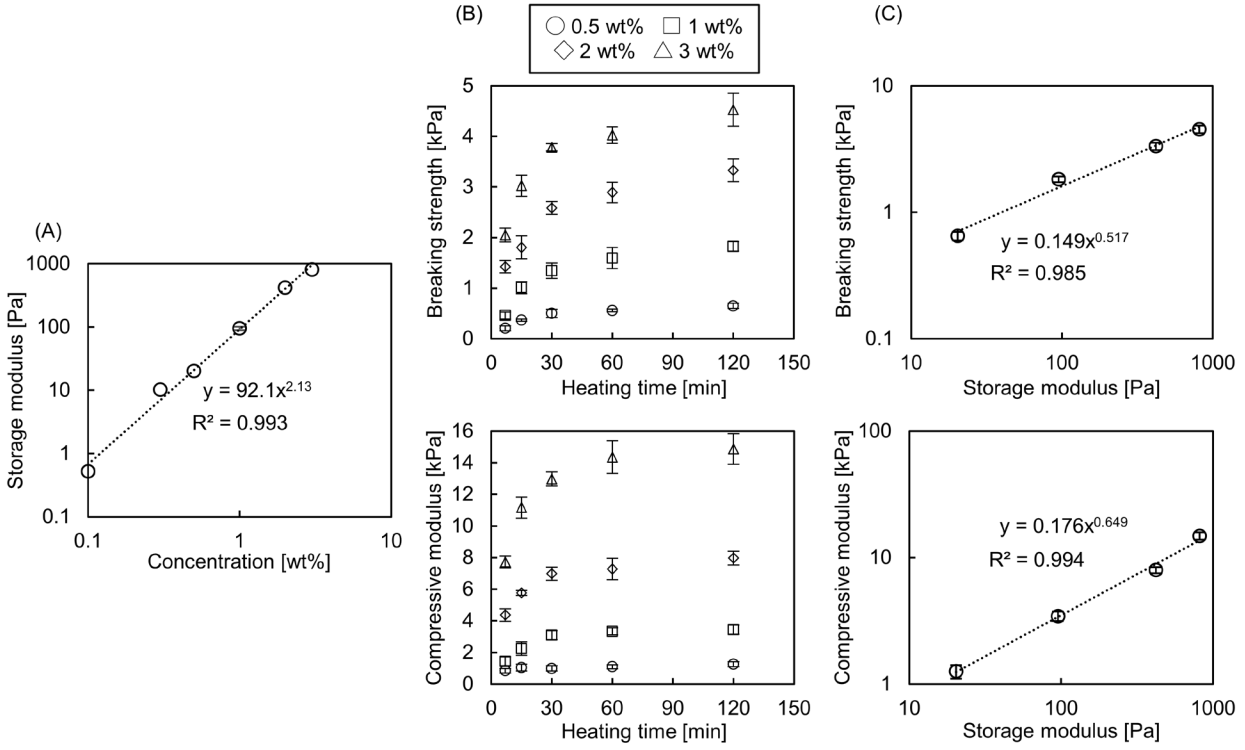

Figure 7. (A) Storage modulus of CNF dispersions subjected to 50 passes at an angular frequency of 1.26 s^{-1} plotted as a function of cellulose concentration. (B) Mechanical strength of CNF hydrogels prepared at various concentrations as a function of heating time. (C) Mechanical strength of CNF hydrogels as a function of storage modulus (the mechanical strengths correspond to those of the hydrogels heated for 120 min in Figure 7B). In Figure 7A, the error bars show standard deviation; the measurements were performed in triplicate. In Figure 7B and 7C, the error bars show standard deviation; the measurements were performed in quintuplicate.

Various relationships between storage modulus and concentration in CNF suspensions have been identified, one of which is expressed in Equation 4.[31]

$$G' \propto kc^{\alpha}, \qquad \text{Eq. 4}$$

where G' is the storage modulus, k is a front factor proportional to the Young's modulus and the square of the axial ratio of a single fiber, and α is value dependent on the network structure. It has been reported that α equals 2.25 in a random 3D polymer network.[31] Therefore, the CNF dispersions analyzed in this study exhibited structural features similar to those reported for a random 3D-network. Photographs of hydrogels prepared with various CNF concentrations are shown in Figure S7. Although the network structure in dispersions containing >0.1 wt.% CNF consisted of entangled NFs, the gelation of 0.1 wt.% CNF suspensions generated flowing dispersions, while gelation of 0.3 wt.% CNF dispersions resulted in collapse and the expulsion of water.

The storage modulus was a more important factor for sufficient gelation than network structure. Sufficient gelation was achieved when the storage modulus of the CNF dispersion exceeded 20 Pa. Indeed, the storage modulus of the 1 wt.% CNF dispersion subjected to 5 passes was 29.5 Pa (Figure 5B), and that of the 0.5 wt.% CNF dispersion subjected to 50 passes was 20.3 Pa (Figure 7A). The mechanical strengths of the CNF hydrogels made with various CNF concentrations are plotted against heating times in Figure 7B. The mechanical strength of the CNF hydrogels increased with increasing CNF concentration and heating time. This was attributed to development of the network structure of interconnected NFs. The dependence of mechanical strength on the storage modulus is illustrated in Figure 7C; the mechanical strengths of the hydrogels heated for 120 min from Figure 7B are plotted against the storage moduli for the corresponding concentrations from Figure 7A. The slopes of

the plots of breaking strength vs. storage modulus and compressive modulus vs. storage modulus had gradients of 0.52 and 0.65, respectively. Even though the density of NF entanglement increased significantly with increasing CNF concentration (Figure 7A), the magnitude of the increase in mechanical strength relative to the storage modulus was small. These results showed that not all of the points of entanglement between the NFs could be converted to adhesion points by hydrothermal treatment. Increasing the conversion of entanglement points to adhesion points will enhance the mechanical strength of the resulting hydrogels. Thus, future preparation methods should be carefully planned.

4. CONCLUSIONS

CNF dispersions were converted to self-sustaining hydrogels by hydrothermal treatment at 160 °C without chemical modification. The NF width increased with heating time, which was due to adhesion between the CNFs. The network structure that formed retained water within its framework, which resulted in gelation. The chemical and crystal structures of the CNFs were unchanged following hydrothermal gelation. In addition, no discoloration indicative of caramelization was observed. On the other hand, some organic acids were formed through hydrolysis of the saccharides, which reduced the pH of the affected hydrogels to approximately 5. The results of SEC and light scattering analysis also suggested some hydrolysis of the cellulose polymer, and the DP_w of the hydrogels decreased from 320 to 260 as the heating time increased. The plots of molecular mass vs. elution volume did not shift toward higher molecular mass. This indicated that crosslinking through hemiacetal or ester linkages did not occur between cellulose polymers. From these results, we concluded that the CNF hydrogels formed via hydrothermal treatment were physical gels, and that the network structure may have

formed through simple attractive forces, such as van der Waals forces.

The influence of disintegration time and CNF concentration on the mechanical strength of the CNF hydrogels was also investigated. Increasing the number of passes produced NFs of reduced width and length, which aided the development of network structures in the dispersions. Because gelation occurred via adhesion at points of entanglement, the more developed network structures provided greater mechanical strength. The network structure was more developed when using more concentrated CNF dispersions. Below 0.3 wt.% CNF, the network structure was unable retain water, which caused the hydrogels to flow following hydrothermal treatment. However, with a CNF concentration above 0.5 wt.%, the resulting hydrogels had self-sustaining structures. Interestingly, an important condition for hydrothermal gelation was the use of CNF dispersions with >20 Pa storage moduli rather than CNF dispersions with extensively networked structures.

ASSOCIATED CONTENT

Supporting Information. Supporting Information is available on the ACS Publications website at DOI: _____

The following files are available free of charge.

Photographs of the CNF hydrogels prepared at 1 wt.% with various disintegration times and heating times (Figure S1); UV-visible transmittance spectra of the CNF dispersion and hydrogel samples with various heating times, and histograms of NF widths in the CNF hydrogels accompanied by typical FE-SEM images (Figure S2); overlapping FTIR spectra without offsets (Figure S3); UV-visible transmittance spectra of the CNF dispersions with various disintegration times, and storage and loss moduli of CNF dispersions with various disintegration times (Figure S4); histograms of NF width and length in the CNF dispersions with various disintegration times

accompanied by typical FE-SEM and AFM images, respectively (Figure S5); storage and loss moduli of CNF dispersions with various concentrations (Figure S6); and photographs the CNF hydrogels prepared at various concentrations with 50 passes and various heating times (Figure S7).

AUTHOR INFORMATION

Corresponding Author

*E-mail: osadam@shinshu-u.ac.jp; Tel.: +81-268-21-5458; Fax: +81-268-21-5391

*ORCID: 0000-0003-3232-5857

Coauthor

E-mail: 17st305g@shinshu-u.ac.jp

ORCID: 0000-0003-2833-3571

Author Contributions

The manuscript was written through contributions of all authors. All authors have given approval to the final version of the manuscript.

Funding Sources

This work was supported by JSPS KAKENHI (grant number 17H04893) and Sasakawa Scientific Research Grant from the Japan Science Society (grant number 2018-3028).

ACKNOWLEDGMENT

We thank Dr. Nobuhide Takahashi, Dr. Hiroshi Fukunaga, Dr. Iori Shimada, Dr. Kazuhide Totani, Dr. Yoshihiro Nomura, and Mr. Kazuhiko Yamashita for their substantial intellectual contributions to the conception of the project.

ABBREVIATIONS

CNF, cellulose nanofiber; DP_n, degree of polymerization by number; DP_w, degree of polymerization by weight; RI, refractive index; CI, crystallinity index; CS, crystal size; FWHM, full width at half-maximum; SEC, size exclusion chromatography; AFM, atomic force microscopy; XRD, X-ray diffraction; FTIR, Fourier-transform infrared.

REFERENCES

(1) Saito, T.; Kimura, S.; Nishiyama, Y.; Isogai, A., Cellulose Nanofibers Prepared by

TEMPO-Mediated Oxidation of Native Cellulose, *Biomacromolecules* **2007**, *8*, 2485–2491.

(2) Fan, Y.; Saito, T.; Isogai, A., Preparation of Chitin Nanofibers from Squid Pen β-Chitin by Simple Mechanical Treatment under Acid Conditions, *Biomacromolecules* **2008**, *9*, 1919–1923.

(3) Ifuku, S.; Nogi, M.; Abe, K.; Yoshioka, M.; Morimoto, M.; Saimoto, H.; Yano, H., Preparation of Chitin Nanofibers with a Uniform Width as α-Chitin from Crab Shells, *Biomacromolecules* **2009**, *10*, 1584–1588.

(4) Mushi, N. E.; Butchosa, N.; Salajkova, M.; Zhou, Q.; Berglund, L. A., Nanostructured Membranes Based on Native Chitin Nanofibers Prepared by Mild Process, *Carbohydr. Polym.* **2014**, *112*, 255–263.

(5) Li, M. C.; Wu, Q.; Song, K.; Cheng, H. N.; Suzuki, S.; Lei, T., Chitin Nanofibers as Reinforcing and Antimicrobial Agents in Carboxymethyl Cellulose Films: Influence of Partial Deacetylation, *ACS Sustainable Chem. Eng.* **2016**, *4*, 4385–4395.

(6) Kose, R.; Mitani, I.; Kasai, W.; Kondo, T., "Nanocellulose" As a Single Nanofiber Prepared from Pellicle Secreted by *Gluconacetobacter xylinus* Using Aqueous Counter Collision, *Biomacromolecules* **2011**, *12*, 716–720.

(7) Watanabe, Y.; Kitamura, S.; Kawasaki, K.; Kato, T.; Uegaki, K.; Ogura, K.; Ishikawa, K., Application of a Water Jet System to the Pretreatment of Cellulose, *Biopolymers* **2011**, *95*, 833–839.

(8) Dutta, A. K.; Izawa, H.; Morimoto, M.; Saimoto, H.; Ifuku, S., Simple Preparation of Chitin Nanofibers from Dry Squid Pen β-chitin Powder by the Star Burst System, *J. Chitin Chitosan Sci.* **2013**, *1*, 186–191.

(9) Oishi, Y.; Nakaya, M.; Matsui, E.; Hotta, A., Structural and Mechanical Properties of Cellulose Composites Made of Isolated Cellulose Nanofibers and Poly(vinyl

alcohol), *Composites, Part A* **2015**, *73*, 72–79.

(10) Suenaga, S.; Osada, M., Self-Sustaining Cellulose Nanofiber Hydrogel Produced by Hydrothermal Gelation Without Additives, *ACS Biomater. Sci. Eng.* **2018**, *4*, 1536–1545.

(11) Suenaga, S.; Osada, M., Parameters of Hydrothermal Gelation of Chitin Nanofibers Determined Using a Severity Factor, *Cellulose* **2018**, *25*, 6873–6885.

(12) Wagner, W.; Pruß, A., The IAPWS Formulation 1995 for the Thermodynamic Properties of Ordinary Water Substance for General and Scientific Use, *J. Phys. Chem. Ref. Data* **2002**, *31*, 387–535.

(13) Segal, L.; Creely, J. J.; Martin, A. E.; Conrad, C. M., An Empirical Method for Estimating the Degree of Crystallinity of Native Cellulose Using the X-Ray Diffractometer, *Text. Res. J.* **1959**, *29*, 786–794.

(14) McCormick, C. L.; Callais, P. A.; Hutchinson, B. H., Solution Studies of Cellulose in Lithium Chloride and *N*,*N*-dimethylacetamide, *Macromolecules* **1985**, *18*, 2394–2401.

(15) Saito, T.; Yanagisawa, M.; Isogai, A., TEMPO-Mediated Oxidation of Native Cellulose: SEC–MALLS Analysis of Water-soluble and -Insoluble Fractions in the Oxidized Products, *Cellulose* **2005**, *12*, 305–315.

(16) Ono, Y.; Ishida, T.; Soeta, H.; Saito, T.; Isogai, A., Reliable d*n*/dc Values of Cellulose, Chitin, and Cellulose Triacetate Dissolved in LiCl/*N*,*N*-Dimethylacetamide for Molecular Mass Analysis, *Biomacromolecules* **2016**, *17*, 192–199.

(17) Nata, I. F.; Wang, S. S. S.; Wu, T. M.; Lee, C. K., β-Chitin Nanofibrils for Self-sustaining Hydrogels Preparation via Hydrothermal Treatment, *Carbohydr. Polym.* **2012**, *90*, 1509–1514.

(18) Lewis, L.; Derakhshandeh, M.;

Hatzikiriakos, S. G.; Hamad, W. Y.; MacLachlan, M. J., Hydrothermal Gelation of Aqueous Cellulose Nanocrystal Suspensions, *Biomacromolecules* **2016**, *17*, 2747–2754.

(19) Langan, P.; Nishiyama, Y.; Chanzy, H., A Revised Structure and Hydrogen-Bonding System in Cellulose II from a Neutron Fiber Diffraction Analysis, *J. Am. Chem. Soc.* **1999**, *121*, 9940–9946.

(20) Langan, P.; Nishiyama, Y.; Chanzy, H., X-ray Structure of Mercerized Cellulose II at 1 Å Resolution *Biomacromolecules* **2001**, *2*, 410–416.

(21) Chang, C.; Zhang, L.; Zhou, J.; Zhang, L.; Kennedy, J. F., Structure and Properties of Hydrogels Prepared from Cellulose in NaOH/Urea Aqueous Solutions, *Carbohydr. Polym.* **2010**, *82*, 122–127.

(22) Shen, X.; Shamshina, J. L.; Berton, P.; Bandomir, J.; Wang, H.; Gurau, G.; Rogers, R. D., Comparison of Hydrogels Prepared with Ionic-Liquid-Isolated vs Commercial Chitin and Cellulose, *ACS Sustainable Chem. Eng.* **2016**, *4*, 471–480.

(23) Antal, M. J.; Mok, W. S. L.; Richards, G. N., Mechanism of Formation of 5-(Hydroxymethyl)-2-furaldehyde from d-Fructose and Sucrose, *Carbohydr. Res.* **1990**, *199*, 91–109.

(24) Bobleter, O., Hydrothermal Degradation of Polymers Derived from Plants, *Prog. Polym. Sci.* **1994**, *19*, 797–841.

(25) Kabyemela, B. M.; Adschiri, T.; Malaluan, R. M.; Arai, K., Glucose and Fructose Decomposition in Subcritical and Supercritical Water: Detailed Reaction Pathway, Mechanisms, and Kinetics, *Ind. Eng. Chem. Res.* **1999**, *38*, 2888–2895.

(26) Aida, T. M.; Yamagata, T.; Abe, C.; Kawanami, H.; Watanabe, M.; Smith, R. L., Production of Organic Acids from Alginate in High Temperature Water, *J. Supercrit. Fluids* **2012**, *65*, 39–44.

(27) Hiraoki, R.; Ono, Y.; Saito, T.; Isogai,

A., Molecular Mass and Molecular-Mass Distribution of TEMPO-Oxidized Celluloses and TEMPO-Oxidized Cellulose Nanofibrils, *Biomacromolecules* **2015**, *16*, 675–681.

(28) Sugiyama, J.; Vuong, R.; Chanzy, H., Electron Diffraction Study on the Two Crystalline Phases Occurring in Native Cellulose from an Algal Cell Wall, *Macromolecules* **1991**, *24*, 4168–4175.

(29) Kondo, T.; Kose, R.; Naito, H.; Kasai, W., Aqueous Counter Collision Using Paired Water Jets as a Novel Means of Preparing Bio-nanofibers, *Carbohydr. Polym.* **2014**, *112*, 284–290.

(30) Suenaga, S.; Osada, M., Systematic Dynamic Viscoelasticity Measurements for Chitin Nanofibers Prepared with Various Concentrations, Disintegration Times, Acidities, and Crystalline Structures, *Int. J. Biol. Macromol.* **2018**, *115*, 431–437.

(31) Yu, L.; Tatsumi, D.; Morita, M., Relationship between Viscoelasticity and Electrical Conductivity of Carbonized Cellulose Fiber Networks, *Nihon Reoroji Gakkaishi* **2013**, *41*, 331–336.

Table of Contents